# Photometric properites of the surface of Io and their influence on line formation in the atmosphere

by

Yuk L. Yung and Richard M. Goody

Center for Earth and Planetary Physics,
Harvard University.



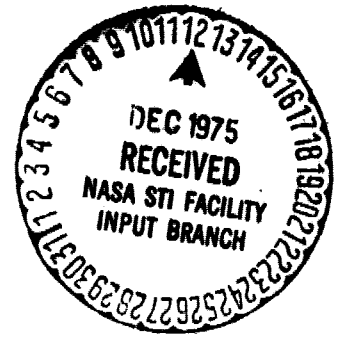

## Abstract

We give a quantitative theory of line formation in an atmosphere above a surface with backscattering properties. Sufficiently high spatial and spectral resolution spectra of resonance lines in Io region A can yield data on the surface scattering properties as well as the number density of scattering molecules.

We discuss macroscopically homogeneous models of scattering from the surface of Io and conclude that multiple reflection from crystal facets is the most likely cause for the observed phase variations of the geometric albedo.

## 1. Introduction.

Io has a notably high albedo for visible and near infrared radiation. Between 0.5 and 3 μm the geometric albedo of the leading side of the satellite is observed to range from 0.7 to 1.1 (Johnson and McCord, 1970; Johnson, 1971; Johnson and Pilcher, 1974) in contrast to the value 0.67 for a lambert sphere with conservative scattering.

Brown et al. (1975) have pointed out that, for such a high albedo, the sodium D-lines might be observed in absorption, if Region A* alone could be observed.

This effect is important as regards the search for other atomic resonance lines in the atmosphere of Io, and in the first part of this paper we present a quantitative theory. It is apparent from this work that observations of the sodium D-lines in region A could yield information about the photometric properties of the surface of Io as well as the density of sodium atoms in its atmosphere.

In the second part of this paper we give a speculative but quantitative theory for the observed photometric properties of Io's surface. The high geometric albedo implies a scattering function with a stronger backward scattering component than for a lambert surface. This backward scattered component is seen in the phase variation of the albedo at 0.55 μm, which decreases by about 30% from 0° to 12° phase angle (Morrison et al., 1974). In the first part of the paper we treat this component as a narrow bundle of constant intensity, centered on the incident beam.

---

*Region A includes the visible disk and the atmosphere gravitationally bound to the satellite. Sodium D-lines in emission have been observed in regions more distant from the satellite. No spectra from Region A alone are available at the present time.

Enhanced backward scatter is understood for dark surfaces such as lunar material (Hapke, 1963). As pointed out by Oetking (1966) these theories, which involve shadowing effects, cannot be applied to high albedo surfaces, such as Io. Oetking showed that numerous white materials (e.g., MgO) have enhanced backscattering; others, on the contrary, have enhanced scattering at the specular angle (Barkas, 1939). As far as we are able to judge, Öhman (1955) first pointed to the possiblity of cube corners or "cat's eyes" associated with surface crystalline material. He was concerned with the observed negative polarization at small phase angles exhibited by many planetary surfaces, but the same idea can obviously explain enhanced backscattering. Although the exact nature of the reflecting surfaces is unspecified in our model, we believe it to be the only tenable theory for a locally homogeneous surface.

2. Line formation in an atmosphere above a backward scattering surface.

The two models which we shall compare are shown in Figure 1 (a) and (b). For a lambert surface the scattered intensity is the same in every direction. For the backscattering surface, return radiation is restricted to a narrow solid angle ($d\omega$). A real surface, with some backscattering properties, can be approximately represented by a superposition of the two types of surface. The solution for such a surface can be obtained by superposing our two solutions.

The atmosphere in both models scatters isotropically, a close approximation to atomic resonant scattering. We consider only the zero phase intensity $I^{+}(\mu_0, \mu_0)$. (Our notation follows Chandrasekhar, 1960.)

The intensity of radiation of a resonance line formed in a planetary atmosphere is given by the solution of the radiative transfer equation. With standard notation, assuming plane parallel geometry, we have

$$\mu \frac{d I_\lambda(\tau,\mu)}{d\tau} = I_\lambda(\tau,\mu) - \frac{+}{2} \int_{-1}^{1} d\mu' \, I_\lambda(\tau,\mu') \qquad (1)$$

where

$$\tau(\lambda) = \tau_0 \exp\left(-\left(\frac{\lambda-\lambda_0}{\Delta\lambda_D}\right)^2\right)$$

$\tau_0$ = optical thickness at line center

$\Delta\lambda_D$ = Doppler line width

The incident solar beam provides an upper boundary condition:

$$I_\lambda^-(0,\mu,\phi) = \pi F_\lambda \, \delta(\mu-\mu_0)\,\delta(\varphi-\varphi_0) \qquad (2)$$

where $\mu$ and $\mu_0$ are cosines of zenith angles and $\phi$ and $\phi_0$ are azimuthal angles; the subscript zero refers to the sun. For a lower boundary consisting of a lambert surface at $\tau_1$, the reflected radiation is isotropic and the boundary condition can be expressed:

$$I_\lambda^+(\tau_1,\mu,\phi) = \frac{r}{\pi} \int_0^{2\pi} d\phi' \int_0^1 d\mu' \, \mu' \, I_\lambda^-(\tau_1,\mu',\phi') \qquad (3)$$

where $r$ denotes surface reflectivity.

For a backscattering surface, the lower boundary condition is:

$$I_\lambda^+(\tau_1,\mu,\phi) = r \, I_\lambda^-(\tau_1,\mu,\phi) \qquad (4)$$

To make the model more realistic the direct solar beam is dispersed, after scattering by the surface, into a narrow cone of solid angle $d\omega$.

The equation of radiative transfer for the two cases can be solved using the highly accurate approximate technique discussed in Appendix I. For $\tau_1(\lambda) \ll 1$ the solutions assume the following simple expressions for the emergent

intensity $I^{+}_{\lambda}(\mu_0, \mu_0)$ at a point on the surface, and for the geometric albedo, $p(\lambda)$ for a spherical satellite.

Lambert surface:

$$I^{+}_{\lambda}(\mu_0, \mu_0)/F_{\lambda} = \tau\mu_0 + \frac{\tau_1(\lambda)}{4\mu_0}(1 - 2\tau\mu_0)^2 \tag{5}$$

$$p(\lambda) = \frac{2}{3}\tau + \tau_1(\lambda)\left(\frac{1}{8} + \frac{3}{3}\left(\tau - \frac{3}{4}\right)^2\right) \tag{6}$$

Backscattering surface:

$$I^{+}_{\lambda}(\mu_0, \mu_0)/F_{\lambda} = p_0 - \frac{\tau_1(\lambda)}{\mu_0}\left(2\mu_0 - \frac{1}{4}(1+\tau)^2\right) \tag{7}$$

$$p(\lambda) = p_0 - \tau_1(\lambda)\left(4p_0 - \frac{1}{2}(1+\tau)^2\right) \tag{8}$$

where

$$p_0 = \frac{\pi\tau}{d\omega}$$

For $\tau_1 \gg 1$ the influence of the surface is unimportant. The solutions in this case can be given in terms of Chandrasekhar's H-function

$$I^{+}_{\lambda}(\mu_0, \mu_0)/F_{\lambda} = \frac{1}{8} H^2(\mu_0) \tag{9}$$

$$p(\lambda) = \frac{1}{4}\int_0^1 d\mu_0\, \mu_0 H^2(\mu_0) = 0.69 \tag{10}$$

We can understand some features of the formation of an emission or absorption line from an examination of (6) and (8). Let us first discuss (6). Well away from a line center we observe scattered radiation, which we refer to as the continuum. In our models this corresponds to $\tau_1 = 0$ and the geometric albedo is

$$p_{continuum} = \frac{2}{3}\tau$$

Close to a line center (wavelength $\lambda = \lambda_o$), the effect of a thin scattering layer $\tau_1(\lambda)$ results in the formation of a weak <u>emission</u> line. For a nearly white lambert surface, $r \approx 1$, and the contribution of the scattering layer to the geometric albedo is

$$\Delta p = p(\lambda) - p_{continuum} \approx \frac{1}{8} \tau_1(\lambda)$$

A bright lambert surface and a layer of isotropic atomic scatterers are almost equally efficient (or inefficient) in scattering photons in the backward direction, and the atmosphere is very difficult to detect.

The continuum geometric albedo for a backscattering surface is

$$p_{continuum} = p_o = \frac{\pi r}{d\omega}$$

and, for a given value, the surface reflectively $r$ can vary from 0 to 1.0, depending upon the angular spread of the reflected sunlight, $d\omega$. Our solution is only valid, however, for $d\omega$ small. $p_o$ can be large, even for a dark material ($r \to 0$), if $d\omega$ is small. Close to line center ($\lambda = \lambda_o$) the scattering layer $\tau_1(\lambda)$ contributes to the formation of an <u>absorption</u> line if

$$4 p_o - \tfrac{1}{2}(1+r)^2 > 0$$

a condition that will be satisfied for all $r$ if the continuum albedo $p_o$ exceeds 0.5. The observations suggest $d\omega \lesssim 0.15$ and $p \approx 1$; therefore

$$\Delta p = p(\lambda) - p_o \approx -3.5\, \tau_1(\lambda)$$

In this case atmospheric scattering has a much greater effect on the emergent radiation than for a lambert surface. If the observed continuum geometric albedo should be caused half by lambert scattering and half by backscattering the absorption would be nearly thirty times as effective as

the emission.

In the limit of backscattering alone the situation is similar to that of a parallel beam of light traversing a tube containing resonant scatterers. The parallel beam loses intensity. Other directions will gain intensity but this is not measured if only the parallel beam is observed. There is no limb darkening for the backscattering model and the mean air mass is two: two traverses of the atmosphere then lead to the factor 4 on the right hand side of (8). To further illustrate the differences between lambert and backscattering surfaces we show in Figure 2 (a), (b), and (c) a comparison of geometric albedo for the two cases as a function of $\tau_1$ . To bring out the contrast we have chosen the continuum albedo at $\tau_1 = c$ to be 0.67 in all cases. This is accomplished by setting $\gamma = 1$ for the lambert surface and $p_0 = 0.67$ for the backscattering surface. In the case of a backscattering surface we have an additional parameter $\gamma = \frac{p_0 d\omega}{\pi}$, proportional to the spread of the reflected beam. We show results for the cases $\gamma = 0, 0.5$. For the observed values $d\omega = 0.15$, $p \approx 1.0$ we have $\gamma \approx 0.05$. Asymptotically as $\tau_1 \to \infty$ , $p$ approaches the value 0.69, shown in (10). A thick atmosphere will therefore show line reversal. This behavior could, under sutiable circumstances, make it possible to interpret an observed high resolution profile in terms of values for both $\tau_1$ and $\gamma$ .

## 3. A theory for a backscattering surface.

We present an elementary statistical theory for multiple scattering from a surface consisting of microscopic reflecting facets. This is the only way

we have been able to identify in which a homogeneous* surface can give rise to zero-phase geometric albedos in excess of unity.

We have also considered the following possibilities: an amorphous microstructure; multiple refraction at facets; single reflection at facets.

Amorphous microstructure implies isotropic scattering. The geometric albedo for a sphere covered with an optically thick layer of conservative isotropic scatterers is $p = 0.69$ (Equation 10). The question of optical interference between particles (shadowing effect) is a complicated one and has been invoked to explain a strong phase dependence of albedo (Hapke, 1963). The effect is to decrease the albedo below 0.69 for non-zero phase angles rather than to increase it at zero phase.

Multiple refraction at facets can be reduced to the problem of multiple scattering with a phase function corresponding to the average refracted intensity for all orientations of the facets. This phase function will have only forward components, however, and a thick layer of forward scattering particles has a lower zero-phase geometric albedo than a layer of isotropic scatterers.

Finally, in Appendix 2, we offer a simple theory of scattering from a surface by single reflection from mirror facets. The mirror facets all have the same zenith angle but all azimuth angles are allowed, consistent with the assumption of macroscopic homogeneity. The maximum geometric albedo is found when all the mirrors point vertically. Then we have the well-known result for the albedo of a polished sphere, $p = 0.25$.

---

*One of us had the pleasure of discussing with Professor Thomas Gold the possibility of producing the observed geometric albedo by means of surface structures, e.g., mountains, vertical holes, etc. We remain unconvinced that a quantitative theory along these lines is possible but reserve judgement until one is presented.

We therefore consider multiple reflections not only as a plausible mechanism, but, as far as we can judge, the only one capable of giving zero-phase geometric albedos in excess of unity. If the directions of reflecting surfaces are uncorrelated the albedo is no larger than for single reflections. Our model therefore implie correlated facets or, in other words, crystals. Fanale, Johnson and Matson (1974) have postulated the existence of evaporites on the surface of Io for unrelated reasons.

We do not assert that all scattering takes place by reflection at facets. The most likely source of reflections is total internal reflection in dielectric crystals. Only a limited range of orientations of the crystal with respect to the incident beam gives rise to "cat's eyes." Other orientations, which do not lead to total reflection, will exhibit scattering more similar to that from multiple refractions. Moreover, it is hardly likely that the surface of Io is uniformly covered with any single material; indeed, the reflectivity maps of Dollfus and Murray (1974) show that it is not. We therefore picture a mixture of "cat's eyes" and approximations to lambert surfaces; it is the theory of the former which we wish to present.

For completeness we should draw attention to the proposal by Oetking (1966) that enhanced backscattering may be a diffraction effect. The Io phase effect shows neither the rings nor the strong polarization observed in the glory (van de Hulst, 1957, p. 250), and we have, therefore, not considered diffraction further in this paper. Our findings are, however, only applicable to reflecting facets much larger than the wavelength of light.

Reflections from facets as an explanation of observed scattering properties has been considered by Berry (1923), Barkas (1939), and Middleton and Mungall (1952). None of these authors considered multiple reflections. The importance of multiple reflections was, to our knowledge, first pointed out

by Ohman (1955) but he did not present a quantitative theory.

The facets are oriented with respect to the surface with a statistical distribution $M_1(\mu_m)$, where $\mu_m$ is the cosine of the angle between the normals to the surface and the facet. (See Appendix 3 for mathematical details.) The distribution does not depend on the azimuthal angle of the facet and we exclude facets which are oriented "Downwards," i.e., $\mu_m < 0$. Thus for a ray $f(\mu_j, \phi_j)$ to be scattered into the direction $(\mu_i, \phi_i)$ in a single reflection the probability is proportional to $M_1(\mu_m(i,j))$ where

$$\mu_m(i,j) = \frac{\mu_i - \mu_j}{\left[2\left(1-\mu_i\mu_j - (1-\mu_i^2)^{\frac{1}{2}}(1-\mu_j^2)^{\frac{1}{2}}\cos(\phi_i-\phi_j)\right]\right]^{\frac{1}{2}}} \tag{11}$$

is the cosine of the normal of the facet which reflects $f(\mu_j, \phi_j)$ into $f(\mu_i, \phi_i)$. For secondary scattering we introduce a correlation function between the first facet and the second facet, $M_2(\mu_r)$ where $\mu_r$ is the cosine of the angle between the first facet and the second facet. For a ray $f(\mu_k, \phi_k)$ to be scattered into the direction $(\mu_i, \phi_i)$ the probability is proportional to

$$\sum_j M_2(\mu_r(i,j,k))$$

where the sum is over all possible intermediate rays $f(\mu_j, \phi_j)$ and

$$\mu_r(i,j,k) = \frac{\lambda_{ik} - \lambda_{ij} - \lambda_{jk}}{2(\lambda_{ij}\lambda_{jk})^{\frac{1}{2}}}$$

with

$$\lambda_{mn} = 1 - \mu_m\mu_n - (1-\mu_m^2)^{\frac{1}{2}}(1-\mu_n^2)^{\frac{1}{2}}\cos(\phi_m - \phi_n)$$

We represent each function $M_1(\mu_m)$ and $M_2(\mu_m)$ by a gaussian function.

$$\begin{aligned} M_1(\mu_m) &= M_1 \exp\left(-\left(\frac{1-\mu_m}{\sigma_1}\right)^2\right) \\ M_2(\mu_r) &= M_2 \exp\left(-\left(\frac{\mu_r}{\sigma_2}\right)^2\right) \end{aligned} \tag{12}$$

where $M_1$ and $M_2$ are constants to be determined by normalization conditions.

The emergent angles are denoted by $\epsilon$ and $\phi$; the latter refers to the angle between the planes containing the incident and the emergent rays. Each scattering diagram is normalized by

$$\int_0^{2\pi} d\phi_\epsilon \int_0^1 d\mu_\epsilon \, f(\mu_\epsilon, \phi_\epsilon ; \mu_i, \phi_i) = 1 \qquad (13)$$

In Figure 3 we show calculations of the scattering diagrams for a correlated mirror surface for three angles of incidence and for $\sigma_1 = 10$, $\sigma_2 = 0.1$. This implies that individual facets are distributed at random to the surface normal but that a correlation exists between pairs such that a related mirror is probably to be found within $\pm$ 0.1 radians. Not unexpectedly, the scattering diagrams reveal a backscattering peak with a width of about 30°–40° superposed on a more uniform diffuse reflection.

These results can be used to calculate the geometric albedo and its variation with solar phase, $\alpha$. We assume that the reflected intensity, I, has the simple form

$$I(\mu_\epsilon, \phi_\epsilon ; \mu_i, \phi_i) = B \mu_i^k \mu_\epsilon^{k-1} f(\mu_\epsilon, \phi_\epsilon ; \mu_i, \phi_i) \qquad (14)$$

where B and k are the Minnaert constants (see, for example, Veverka, 1974). Note that B and k are not taken to be functions of $\alpha$ since this functional dependence is already accounted for by the scattering function for a surface element, $f(\mu_\epsilon, \phi_\epsilon ; \mu_i, \phi_i)$. $k$ is a measure of limb-darkening; $k = 0$ and $k = 1$ correspond to cases of zero and lambert limb-darkening respectively. B sets the absolute reflectivity of a spherical surface, i.e., the bond albedo, A. For our present investigation we choose $A = 1$ and have calculated two cases $k = 0$ and $k = 1$. The resulting geometric albedo and its variation are calculated by the method outlined by Horak (1950). The geometric albedos for the two cases are 1.49 and 2.00 respectively. The phase variation $\Phi = \frac{p(\alpha)}{p(0)}$ is

shown in Figure 4, and the result indicates that the phase variation of Io is better described by our model than by a lambert surface. We have meager evidence to distinguish between the cases $k = 0$ and 1 since spatial resolution of the surface of Io would be needed for the task. However, from the isophotes of Io taken by Dollfus and Murray (1974) we must conclude that Io does not exhibit limb-darkening, except perhaps towards the polar caps. Thus we would be inclined to favor the choice of $k = 0$.

The parameter $\bar{\sigma}_2$ is critical for determining the width of the backscattered peak. The width varies in proportion to $\bar{\sigma}_2$ while the height of the peak and the zero phase geometric albedo vary approximately in inverse proportion. Thus geometric albedos in excess of 2.0 are possible, depending upon the nature of the surface.

In actuality we anticipate a mixture of backscattering and lambert surfaces on Io, each with a reflectivity less than one. Until more is known about the surface, it is difficult to unravel the number of parameters involved. The purpose of the present calculation is to demonstrate the properties of multiple reflections from facets, and to show that this is a plausible model for the observed photometric properties of Io.

Acknowledgements

We wish to acknowledge support under grant DES 72-01472 A03 from the Atmospheric Sciences Section of the National Science Foundation, and under grant NGL 22-007-228 from the National Aeronautics and Space Agency. One of us (Y. Y.) also acknowledges support by Kitt Peak National Observatory under NASA Contract NAS 7-100.

## Figure Captions

Figure 1. Geometry for radiative transfer.

In (a) the surface reflects incident radiation according to lambert's law. Case (b) is for a backscattering surface.

Figure 2. Geometric albedo in the neighborhood of a line center.

For the lambert surface the reflectivity is chosen to be 1.0 so that the continuum geometric albedo is 2/3. For the backscattering surface the continuum albedo $p_c = \frac{\pi r}{d\omega}$ is chosen to be 2/3. We show two representative cases $(r, d\omega) = (0.5, 2.4); (0,0)$. $\tau_1$ is the optical thickness of the scattering layer at line center $\lambda = \lambda_c$ (a) $\tau_1 = 3.0$; (b) $\tau_1 = 1.0$; (c) $\tau_1 = 0.1$.

Figure 3. Scattering diagrams for a surface consisting of correlated mirror facets.

The angles $i$ and $\epsilon$ are respectively the zenith angles of the incident and emergent rays. $\phi$ is the azimuthal angle between the plane containing the incident ray and the plane containing the emergent ray and the surface normal. (a), (b) and (c) illustrate the results for three angles of incidence: $i = 6.7°$, 33°, and 59°. The parameters $\sigma_1$ and $\sigma_2$ equal 10 and 0.1 respectively; $f$ is normalized such that $\int d\omega_\epsilon f(\mu_\epsilon, \phi_\epsilon ; \mu_i, \phi_i) = 1$

Figure 4. Phase variation of the geometric albedo.

The scattering diagram shown in Figure 3 is used for $k=0$ and $k=1$, as explained in the text. The geometric albedos for the two cases are 1.49 and 2.00 respectively, for conservative scattering. The result shows the behavior of the measured phase variation from 0° to 12° (Morrison et al., 1974).

Figure A1. Single reflection by a sphere covered with mirror facets.

(a) Reflecting cones in the torus $\theta \pm \delta\theta$

(b) Reflection by a surface element of a cone.

Figure A2. Schematic diagrams for multiple scattering by mirror facets.

(a) Vector representation of incident and emergent rays, and mirror facets.

(b) Dispersion of incident ray due to variation in $\underset{\sim}{m}_{ij}$.

(c) Multiple scattering by mirror facets to Nth order.

Appendix 1: Calculation of emergent intensity and geometric albedo.

We solve the equation of radiative transfer (1) for lambert and backscattering surfaces. The incident solar beam enters a scattering layer of optical thickness $\tau_1$ at zenith angle $\cos^{-1}\mu_0$ and an azimuthal angle $\phi_0$ (Figure 1.). For simplicity we will not carry along the index $\lambda$ in (1). Define the source function

$$J(\tau) = \frac{1}{4\pi} \int_0^{2\pi} d\phi \int_{-1}^{1} d\mu \, I(\tau, \mu, \phi) \tag{A1}$$

$I(\tau, \mu, \phi)$ can be expressed formally in terms of $J(\tau)$ (Chandrasekhar, 1960, p. 12) as

$$I^+(\tau, \mu, \phi) = I^+(\tau_1, \mu, \phi)\, e^{-(\tau_1-\tau)/\mu} + \int_\tau^{\tau_1} \frac{ds}{\mu}\, e^{-(s-\tau)/\mu} J(s) \tag{A2}$$

$$I^-(\tau, \mu, \phi) = I^-(0, \mu, \phi)\, e^{-\tau/\mu} + \int_0^{\tau} \frac{ds}{\mu}\, e^{-(\tau-s)/\mu} J(s) \tag{A3}$$

At the upper boundary $\tau=0$ we have

$$I^-(0, \mu, \phi) = \pi F \, \delta(\mu-\mu_0)\, \delta(\phi-\phi_0) \tag{A4}$$

At the lower boundary $\tau=\tau_1$ we have, for a lambert surface,

$$I^+(\tau_1, \mu, \phi) = \frac{r}{\pi} \int_0^{2\pi} d\phi' \int_0^{1} d\mu' \, \mu' \, I^-(\tau_1, \mu', \phi') \tag{A5}$$

and for a backscattering surface,

$$I^+(\tau_1, \mu, \phi) = r \, I^-(\tau_1, \mu, \phi) \tag{A6}$$

Substituting (A2)-(A3) into (A1) and making use of (A4)-(A6) we obtain an integral equation for the source function

$$J_\ell(\tau, \mu_0) = \left(\frac{1}{4} + \frac{1}{2}\mu_0 r E_2(\tau_1-\tau)\right) e^{-\tau/\mu_0} F + \int_0^{\tau_1} ds \left(\frac{1}{2} E_1(|\tau-s|) + r E_2(\tau_1-\tau)\, E_2^{(A7)}(\tau_1-s)\right) J(s, \mu_0)$$

for a lambert surface and

$$J_{bs}(\tau,\mu_0) = \tfrac{1}{4}\left(e^{\tau/\mu_0} + r\, e^{-(2\tau_1-\tau)/\mu_0}\right) + \tfrac{1}{2}\int_0^{\tau_1} ds\left(E_1(|\tau-s|) + r\,E_1(2\tau_1-\tau-s)\right) J(s,\mu_0) \quad \text{(A8)}$$

for a backscattering surface, where the function $E_n(x)$ denotes the exponential integral as defined by Chandrasekhar (1960, p. 373). The integral equations (A7) and (A8) can be solved iteratively on a computer. However, using a combination of variational and iterative techniques developed by Sze (1975), we can readily obtain approximate analytic solutions for the source functions

$$J_\ell(\tau,\mu_0) \quad \text{and} \quad J_{bs}(\tau,\mu_0)$$

Using (A2) we can compute the emergent intensity $I^+(\mu_0,\mu_0)$ in the direction $\mu$. For the outer solar system we are always close to zero solar phase angle and the most interesting quantity is $I^+(\mu_0,\mu_0)$ given by

$$I^+_\ell(\mu_0,\mu_0)/F = r\mu_0\, e^{-2\tau_1/\mu_0} + \int_0^{\tau_1} \frac{d\tau}{\mu_0}\left(e^{-\tau/\mu_0} + 2r\,E_1(\tau_1-\tau)\right) J(\tau,\mu_0) \quad \text{(A11)}$$

$$I^+_{bs}(\mu_0,\mu_0)/F = \frac{r\pi}{d\omega}\, e^{-2\tau_1/\mu_0} + \int_0^{\tau_1} \frac{d\tau}{\mu_0}\left(e^{-\tau/\mu_0} + r\, e^{-(2\tau_1-\tau)/\mu_0}\right) J(\tau,\mu_0) \quad \text{(A12)}$$

The geometric albedo of Io can be calculated from the equation

$$p = \frac{2\pi \int_0^1 d\mu_0\, \mu_0\, I^+(\mu_0,\mu_0)}{\pi F}$$

Appendix 2: Geometric albedo for a sphere covered with mirror facets: single scattering

The only restriction comes from the assumption of local homogeneity. This requires that the mirror distribution be symmetrical with respect to the local vertical. Take one local vertical at a time. To maintain symmetry the mirrors must be formed into a cone of revolution. We shall assume that the mirrors are inclined at an angle $\theta$ with respect to the local horizon. If all the cones within the torus $\theta \pm \delta\theta$ reflect backwards, the area of the reflecting surface, as shown in figure A1-a is

$$4\pi r^2 \cos\theta \sin\theta \, \delta\theta$$

The reflected light is spread $4\delta\theta$. Consider the fraction of each cone reflecting (see figure A1-b). If all the light within the slice $2\delta\phi$ is back reflected, the fraction is $\delta\phi$. The angular deviation is $4\delta\phi \sin\theta$. Thus the total reflecting area is

$$4\pi r^2 \cos\theta \sin\theta \, \delta\theta \, \delta\phi$$

and the total angular deviation is

$$4(\delta\theta + \delta\phi \sin\theta)$$

The corresponding solid angle of dispersion is

$$d\omega = 4\pi (\delta\theta + \delta\phi \sin\theta)^2$$

From the definition of geometric albedo we have

$$p = \frac{4 \cos\theta \sin\theta \, \delta\theta \, \delta\phi}{4(\delta\theta + \delta\phi \sin\theta)^2}$$

It would appear that we can choose $\delta\theta$ and $\delta\phi$ independently. But if we impose the condition that illumination is to be uniform inside the bundles we have

$$\delta\phi \sin\theta = \delta\theta$$

so

$$p = \frac{1}{4}\cos\theta$$

In the limit $\theta = 0$, we have the well-known result $p = \frac{1}{4}$, the geometric albedo for a polished sphere.

Appendix 3: Calculation of multiple scattering by correlated mirror facets.

Let us describe a mirror orientation by a unit vector $\underset{\sim}{m}$ perpendicular to its surface. Let the incident and emergent rays be denoted by the unit vectors $\underset{\sim}{a}_j$ and $\underset{\sim}{a}_i$ respectively (Figure A2-a). Then the mirror which reflects $\underset{\sim}{a}_j$ into $\underset{\sim}{a}_i$ is characterized by a vector

$$\underset{\sim}{m}_{ij} = \frac{\underset{\sim}{a}_i - \underset{\sim}{a}_j}{\left[2(1-\underset{\sim}{a}_i \cdot \underset{\sim}{a}_j)\right]^{\frac{1}{2}}}$$

If we express $\underset{\sim}{a}_i$ and $\underset{\sim}{a}_j$ in terms of angle variables $(\mu_i, \phi_i)$ and $(\mu_j, \phi_j)$ in polar coordinates we can express $\mu_m(i,j)$ , the cosine of $\underset{\sim}{m}_{ij}$ with respect to the vertical in the form of Eq. (11)

$$\mu_m(i,j) = \frac{\mu_i - \mu_j}{\left[2\left(1-\mu_i\mu_j - (1-\mu_i^2)^{\frac{1}{2}}(1-\mu_j^2)^{\frac{1}{2}}\cos(\phi_i-\phi_j)\right)\right]^{\frac{1}{2}}}$$

For a ray that is scattered twice we have two mirrors $\underset{\sim}{m}_{jk}$ and $\underset{\sim}{m}_{ij}$ . The cosine of the angle between these two vectors is

$$\mu_r(i,j,k) = \underset{\sim}{m}_{ij} \cdot \underset{\sim}{m}_{jk} = \frac{\lambda_{ik} - \lambda_{ij} - \lambda_{jk}}{2\left(\lambda_{ij}\,\lambda_{jk}\right)^{\frac{1}{2}}}$$

where

$$\lambda_{mn} = 1 - \mu_m\mu_n - (1-\mu_m^2)^{\frac{1}{2}}(1-\mu_n^2)^{\frac{1}{2}}\cos(\phi_m - \phi_n)$$

Suppose we keep the incident ray fixed and vary the vector $\underset{\sim}{m}_{ij}$ within a solid angle $d\omega_m$ (see Figure A2-b). It can be shown that

$$d\omega_i = 4\cos\theta_m\, d\omega_m$$
$$= 4\left(\tfrac{1}{2}(1-\underset{\sim}{a}_i\cdot\underset{\sim}{a}_j)\right)^{\frac{1}{2}} d\omega_m$$

Let the incident solar beam be $\bar{f}(\mu_0, \phi_0)$. In the first scattering there is a probability that the ray will be scattered into the upper hemisphere as $f^{\uparrow}(\mu_1, \phi_1)$. This ray will be allowed to escape from the system as an emergent

ray. The part that is scattered into the lower hemisphere $f^-(\mu_1,\phi_1)$ will be scattered a second time. The process will repeat, as shown in Figure A2-c, and the final emergent beam $f^+(\mu,\phi)$ is the sum of all the $f^+(\mu_i,\phi_i)$.

$$f^+(\mu,\phi) = \sum_{i=1}^{\infty} f^+(\mu_i,\phi_i)$$

In each order of scattering we have

$$f(\mu_{i+1},\phi_{i+1}) = \int_0^{2\pi} d\phi_i \int_{-1}^{0} d\mu_i M_1(\mu_{i+1},\phi_{i+1};\mu_i,\phi_i)\, f^-(\mu_i,\phi_i)$$

$M_1(\mu_m)$ is normalized to

$$\int_0^{2\pi} d\phi_{i+1} \int_{-1}^{1} d\mu_{i+1}\; M_1(\mu_{i+1},\phi_{i+1};\mu_i,\phi_i) = 1$$

The conservative nature of scattering follows from

$$\int_0^{2\pi} d\phi_{i+1} \int_{-1}^{1} d\mu_{i+1}\, f(\mu_{i+1},\phi_{i+1}) = \int_0^{2\pi} d\phi_i \int_{-1}^{0} d\mu_i\; f^-(\mu_i,\phi_i)$$

For correlated mirror facets we introduce a correlation function $M_2(\mu_r)$. Let

$$d\omega_i = d\mu_i\, d\phi_i$$

$$f(\mu_2,\phi_2) = \int d\omega_1 M_1(\mu_2,\phi_2;\mu_1^-\phi_1)\, M_2(\mu_2\phi_2;\mu_1^-\phi_1;\mu_0^-\phi_0)\, f(\mu_0^-,\phi_0)$$

where $\mu_i^-$ denotes a beam in the lower hemisphere. Normalization is assured by

$$\int d\omega_2\, M_2(\mu_2\phi_2;\mu_1^-\phi_1;\mu_0^-\phi_0)\, M_1(\mu_2\phi_2,\mu_1^-\phi_0) = 1$$

Again, the system is conservative. Similarly we can compute a higher order scattering

$$f(\mu_3,\phi_3) = \int d\omega_2 M_1(\mu_3,\phi_3;\mu_2^-,\phi_2) \int d\omega_1 M_1(\mu_2^-,\phi_2;\mu_1^-,\phi_1)\, f(\mu_1^-,\phi_1) \times M_2(\mu_3\phi_3;\mu_2^-\phi_2;\mu_1^-\phi_1)$$

$$= \int d\omega_2\, M_2(\mu_3\phi_3;\mu_2^-\phi_2;\mu_1^-\phi_1) M_1(\mu_3\phi_3;\mu_2^-,\phi_2) M_1(\mu_2^-,\phi_2;\mu_1^-,\phi_1)\, f(\mu_1^-,\phi_1)$$

To carry out the calculations numerically we reduce the radiation field to

a set of discrete beams. A frequently occurring integral is of the form

$$S_1(\mu,\phi) = \int_0^{2\pi} d\phi' \int_{-1}^{1} d\mu' \; W(\mu\phi;\mu'\phi')\, S(\mu',\phi')$$

We choose 20 gaussian points for $\mu'$ and 37 equally spaced points for $\phi'$ . The above integration can be approximated by a sum

$$S_1(\mu_k,\phi_\ell) = \sum_{\ell=1}^{37} \sum_{k=1}^{10} a_k b_\ell \; W(k\ell;ij)\, S(\mu_k,\phi_\ell)$$

where we have performed a gaussian quadrature in $\mu'$ and a simpson quadrature in $\phi'$ . The coefficients $a_i$ , $b_j$ refer to the gaussian and simpson weights respectively.

## References


Barkas, W. W. (1939). Analysis of light scattered from a surface of low gloss into its specular and diffuse components. Proc.Phy.Soc.(London), 51, 274-295.

Berry, E. M. (1923). Diffuse reflection of light from a matt surface. J.Opt. Soc. Am., 7, 627-633.

Brown, R. A., Goody, R. M., Murcray, F. J. and Chaffee, F. H., Jr. (1975). Further studies of line emission from Io. Astrophys.J., 200, L49-L53.

Chandrasekhar, W. (1960). Radiative Transfer. Dover Publications, New York.

Dollfus, A. and Murray, B. (1974). La rotation, la cartographie et la photometrie des satellites de Jupiter. Exploration of Planetary Systems (Woszczyk and Iwaniszewska, eds.), 513-525.

Fanale, F. P., Johnson, T. V. and Matson, D. L. (1974). Io:a surface evaporite deposit? Science, 186, 922-925.

Hapke, B. W. (1963). A theoretical photometric function for the lunar surface. J.Geophys.Res., 68, 4571-4586.

Horak, H. G. (1950). Diffuse reflection by planetary atmospheres. Astrophys.J., 112, 445-463.

Johnson, T. V. and McCord, T. B. (1970). Galilean Satellites. The spectral reflectivity 0.30-1.10 micron. Icarus, 13, 37-42.

Johnson, T. V. (1971). Galilean Satellites: Narrowband photometry 0.30 to 1.10 microns. Icarus, 14, 94-111.

Johnson, T. V. and Pilcher, C. B. (1974). Review of satellite spectrophotometry and composition, Planetary Satellites, Proceedings of IAU Colloquium No. 28 (J. Burns, ed.), Cornell Univeristy Press, Ithaca, New York. In press.

Middleton, W. E., and Mungall, A. G. (1952). The luminous directional reflectance of snow. J.Opt.Soc.Am., 42, 572-579.

Morrison, D., Morrison, N. E. and Lazareqicz, A. (1974). Four-color photometry of the galilean satellites. Icarus, 23, 399-416.

Oetking, P. (1966). Photometric studies of diffusely reflecting surfaces with applications to the brightness of the moon. J.Geophys.Res., 71, 2505-2513.

Ohman, Y. (1955). A tentative explanation of the negative polarizaiton in diffuse reflection. Stockholms Obs.Ann., 18-8, 1-10.

Sze, N. E. (1975). Variational methods in radiative transfer problems. J.Rad. Trans.Quant.Spec. To be published.

Van de Hulst, H. C. (1957) Light scattering by small particles. Wiley, New York.

Veverka, J. (1973). The photometric properites of natural snow and of snow-covered planets. Icarus, 20, 304-310.

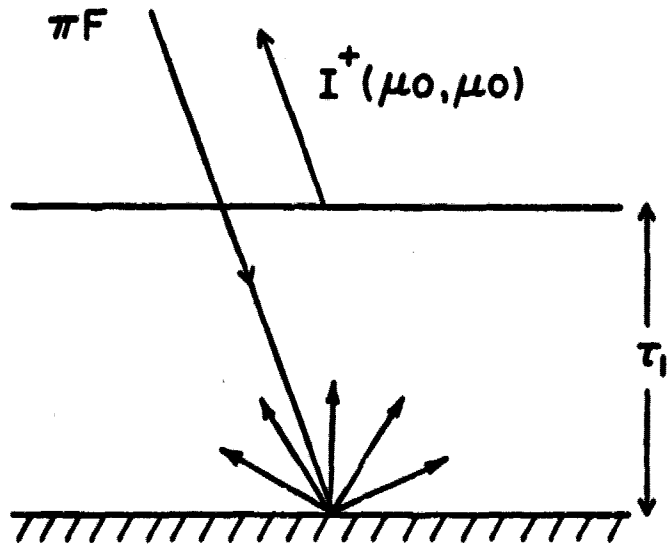


LAMBERT SURFACE

(a)

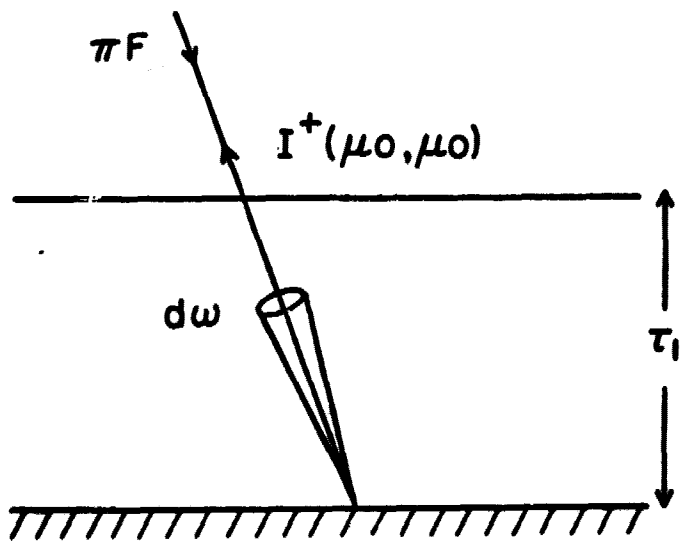


BACKSCATTERING SURFACE

(b)

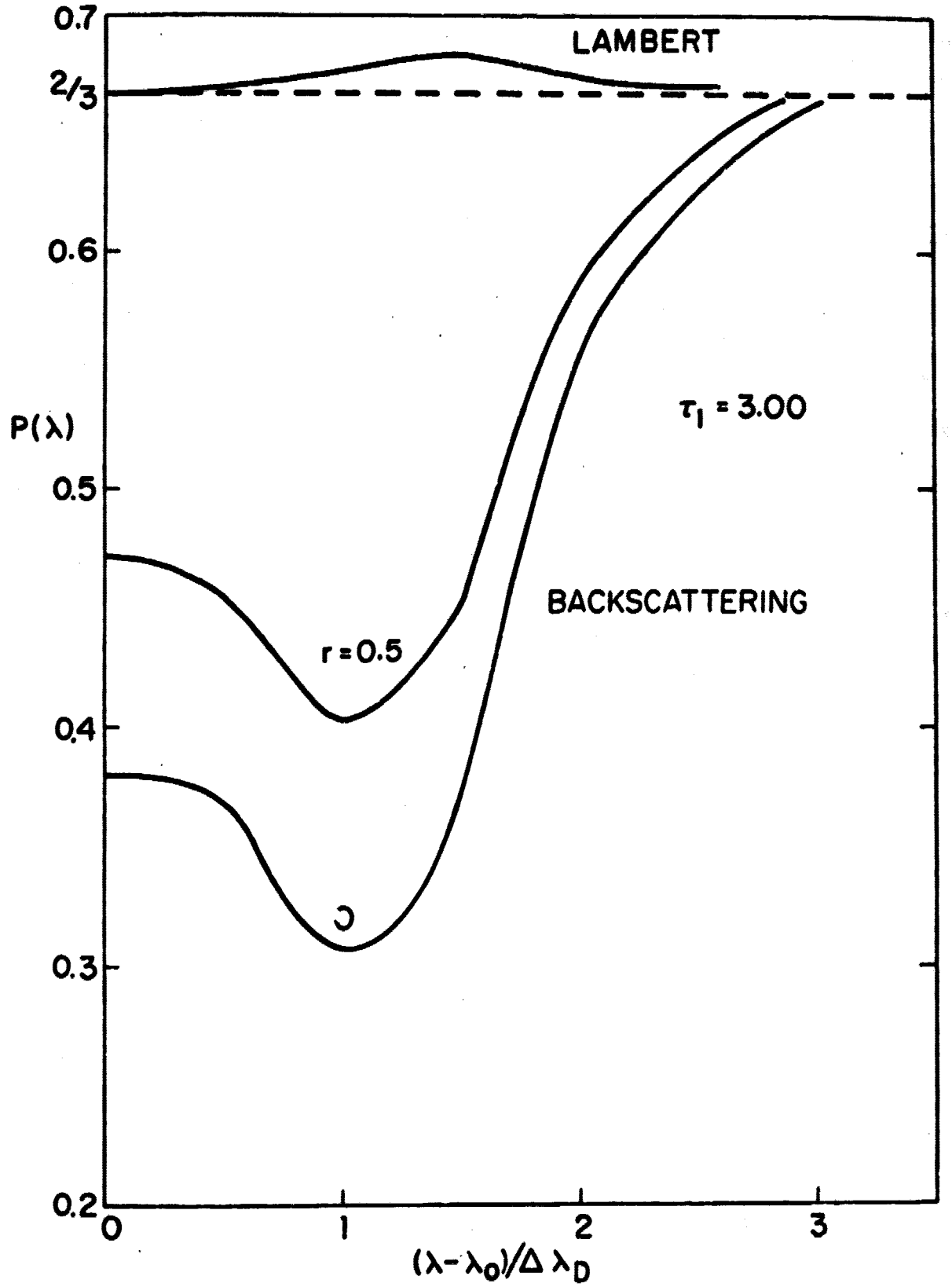
0.7
2/3
0.6
0.5
0.4
0.3
0.2
P(λ)
LAMBERT
τ1 = 3.00
BACKSCATTERING
r = 0.5
0
1
2
3
(λ-λ0)/Δ λD

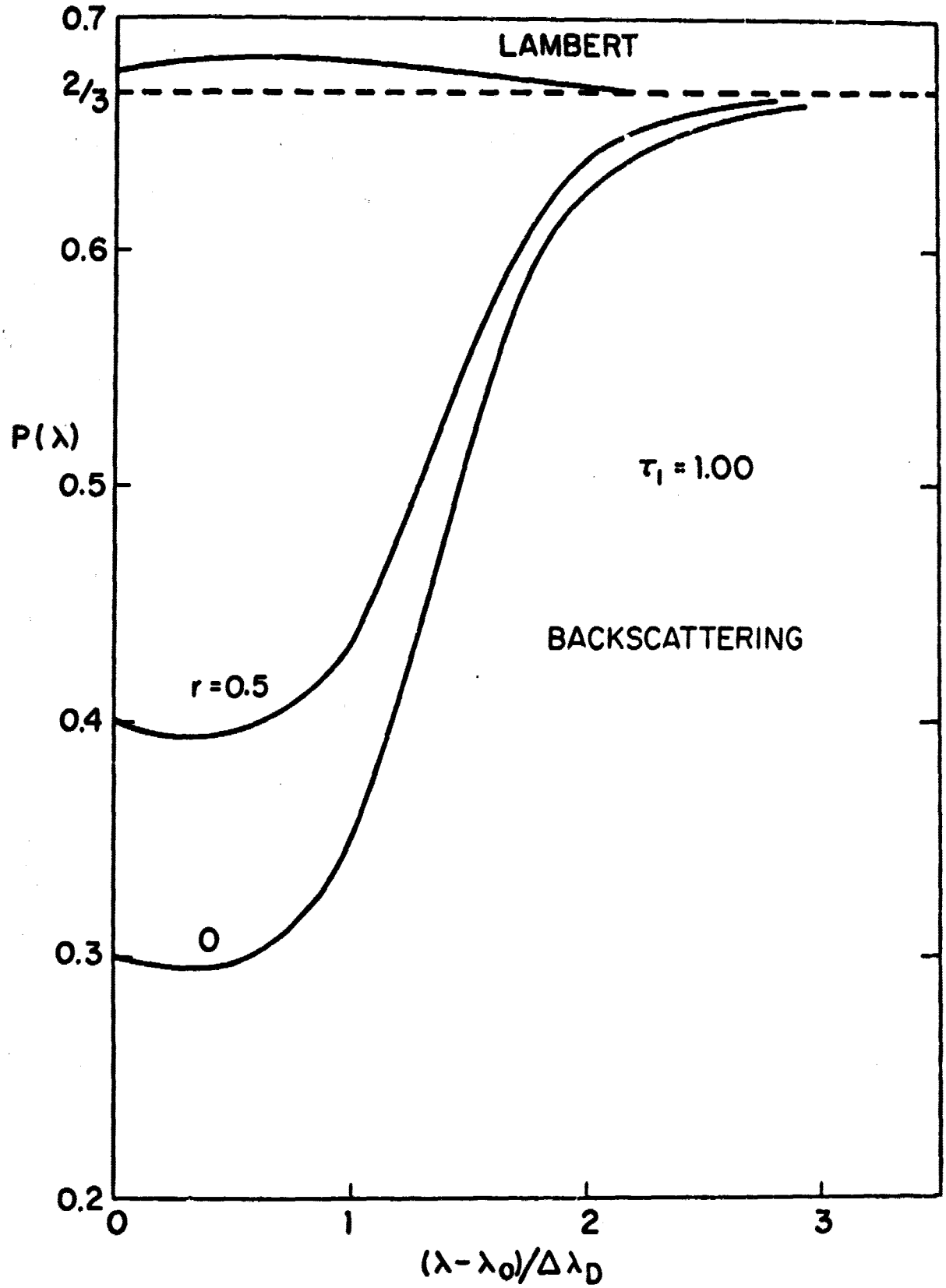
0.7
2/3
0.6
0.5
0.4
0.3
0.2
P(λ)
LAMBERT
τ1 = 1.00
BACKSCATTERING
r = 0.5
0
0
1
2
3
(λ-λ0)/Δλ D

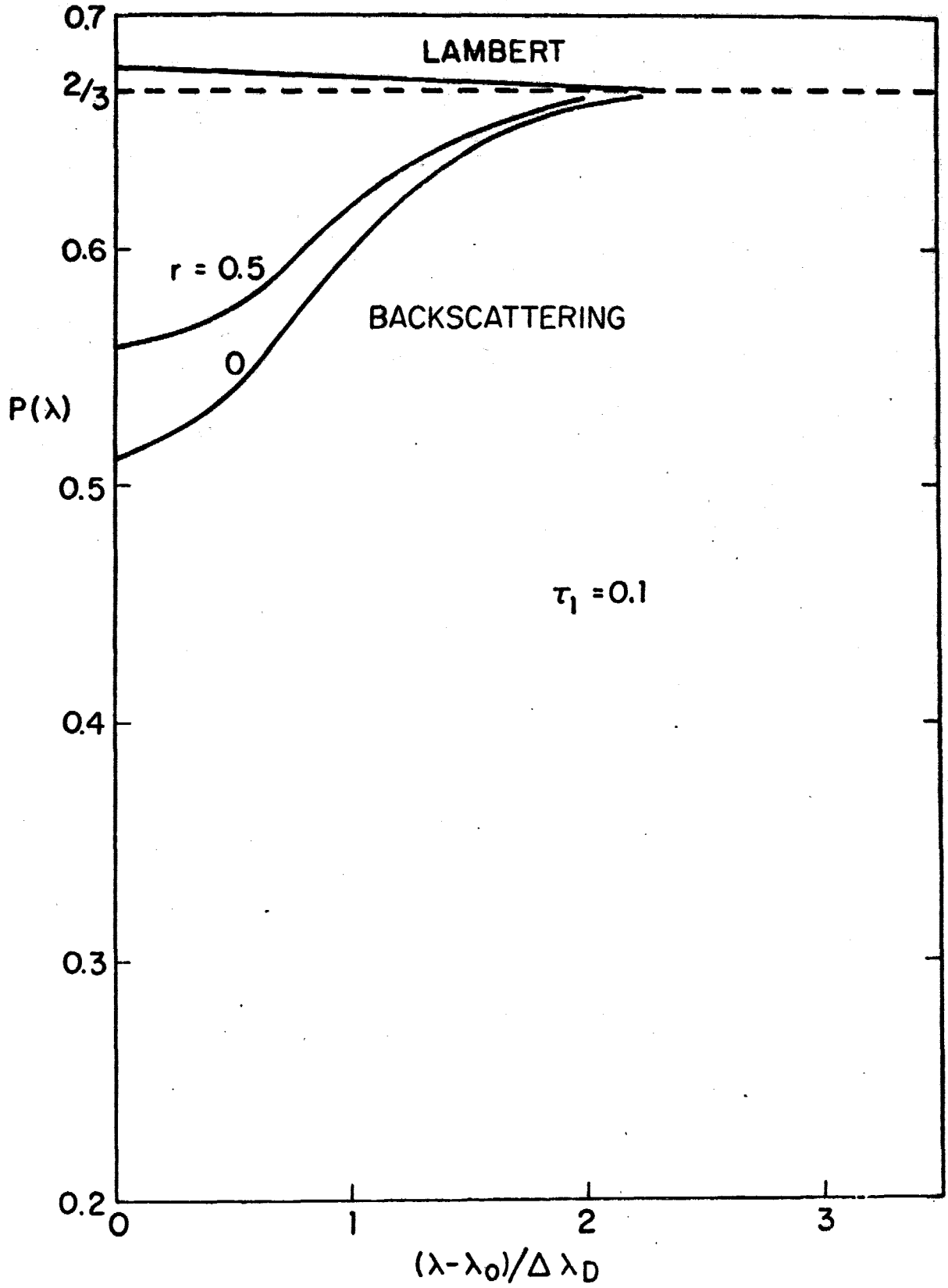
0.7
2/3
0.6
0.5
0.4
0.3
0.2
LAMBERT
r = 0.5
0
BACKSCATTERING
P(λ)
τ1 = 0.1
0
1
2
3
(λ-λ0)/Δ λD

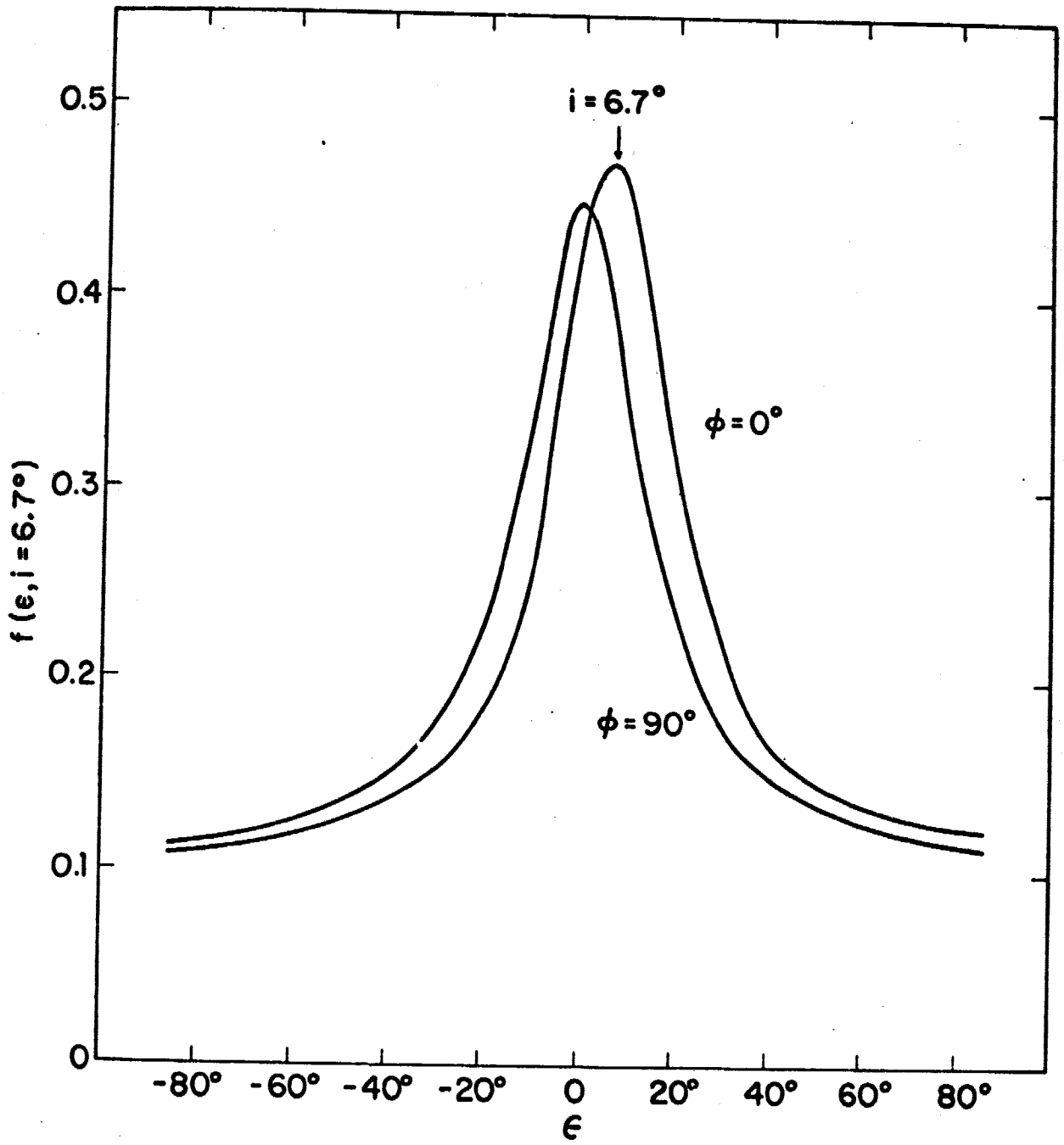
i = 6.7°
φ = 0°
φ = 90°
f(ε, i = 6.7°)
0.5
0.4
0.3
0.2
0.1
0
-80°
-60°
-40°
-20°
0
20°
40°
60°
80°
ε

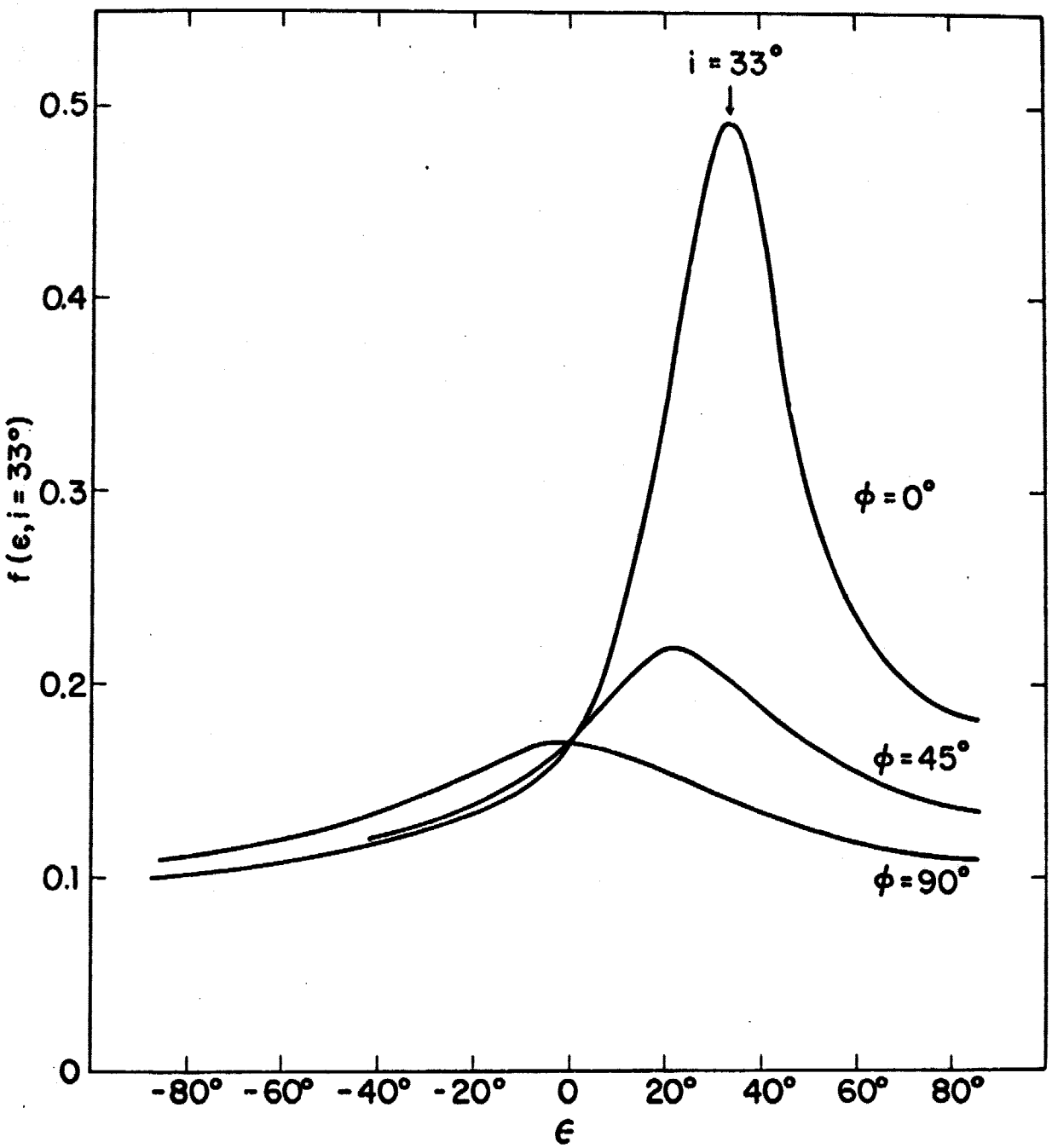
i = 33°
0.5
0.4
0.3
0.2
0.1
0
f(ε, i = 33°)
φ = 0°
φ = 45°
φ = 90°
-80° -60° -40° -20° 0 20° 40° 60° 80°
ε

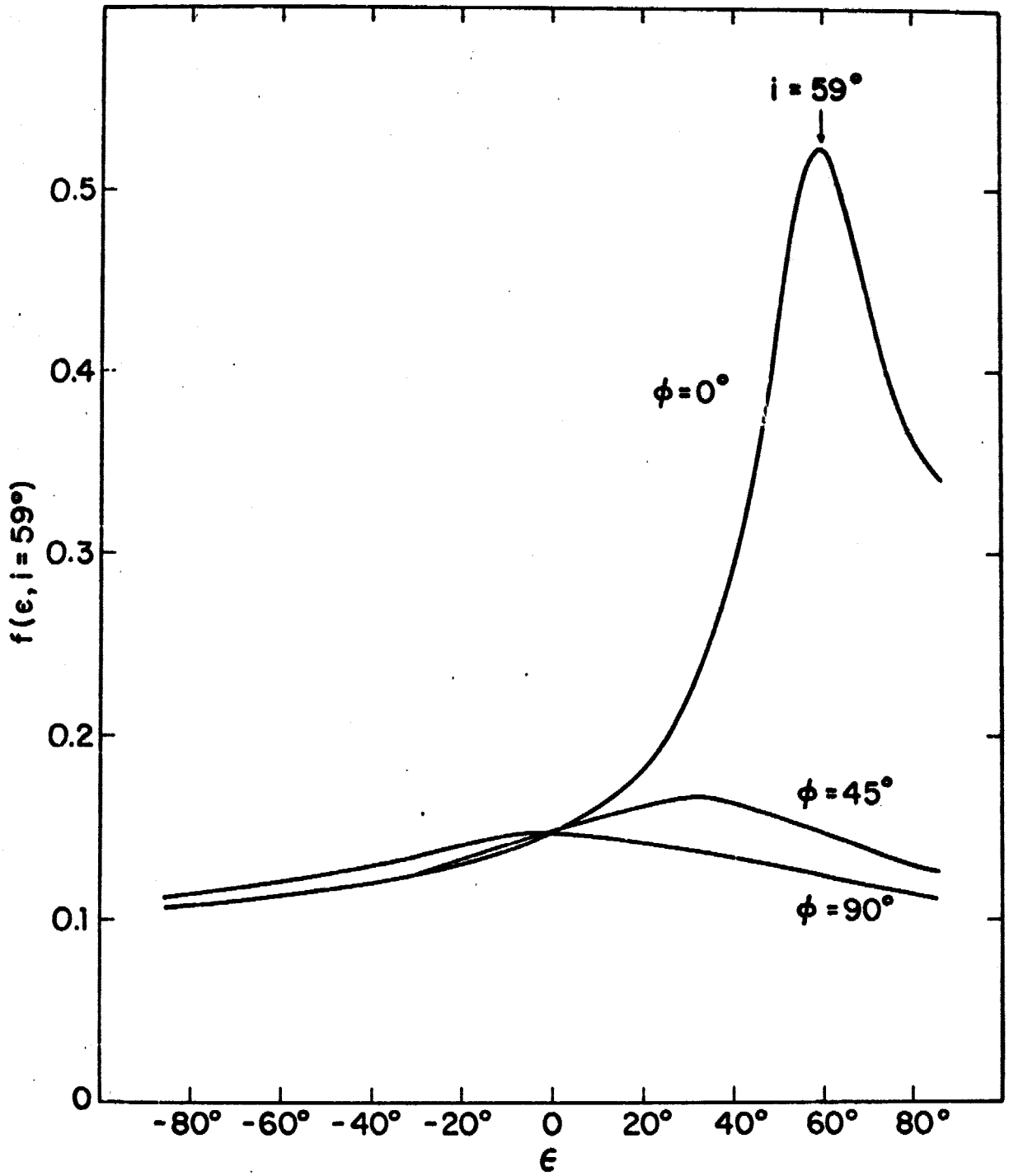
i = 59°
0.5
0.4
0.3
0.2
0.1
0
f(ε, i = 59°)
ϕ = 0°
ϕ = 45°
ϕ = 90°
-80° -60° -40° -20° 0 20° 40° 60° 80°
ε

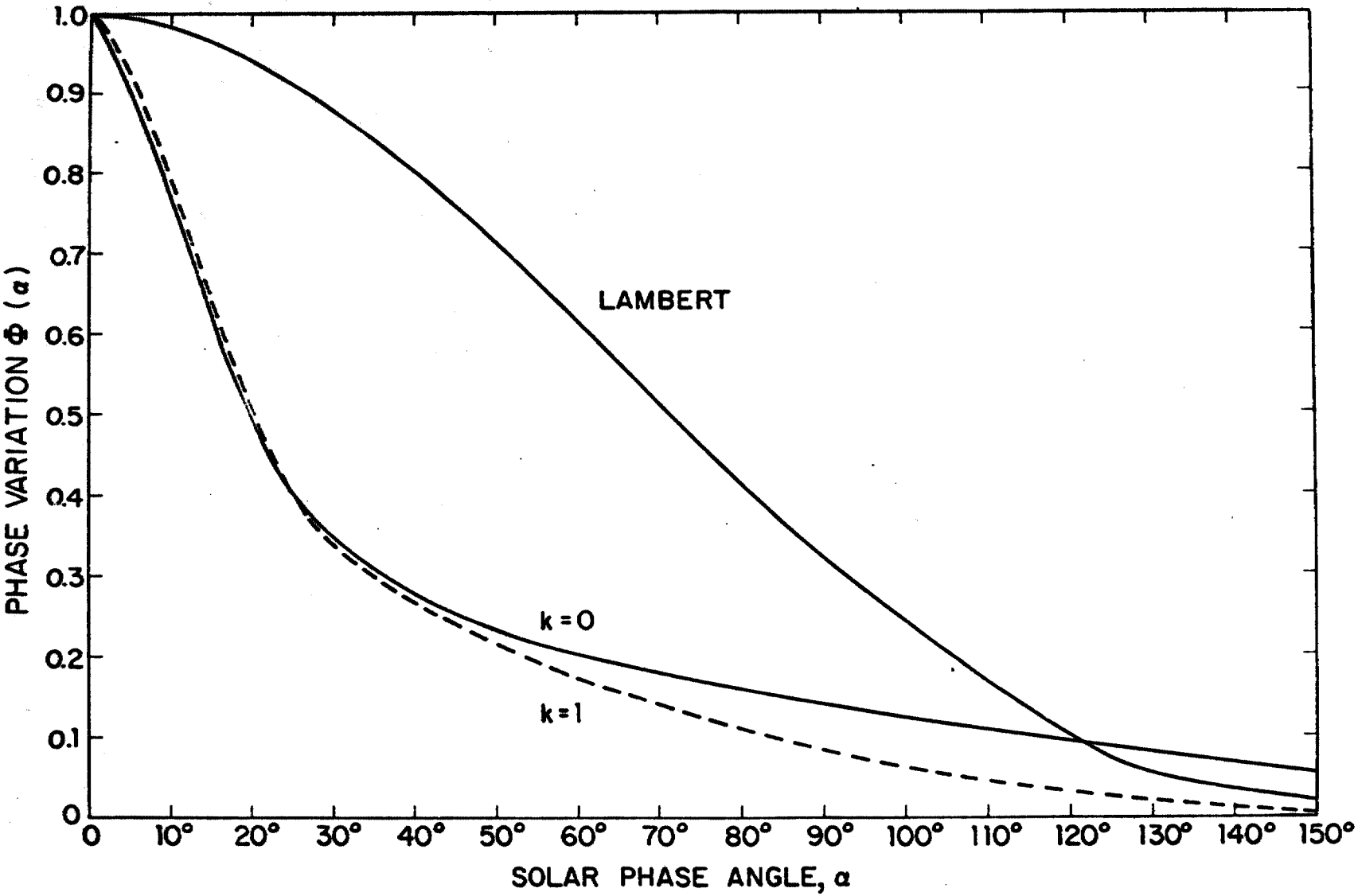
1.0
0.9
0.8
0.7
0.6
0.5
0.4
0.3
0.2
0.1
0
PHASE VARIATION Φ (α)
LAMBERT
k = 0
k = 1
0
10°
20°
30°
40°
50°
60°
70°
80°
90°
100°
110°
120°
130°
140°
150°
SOLAR PHASE ANGLE, α

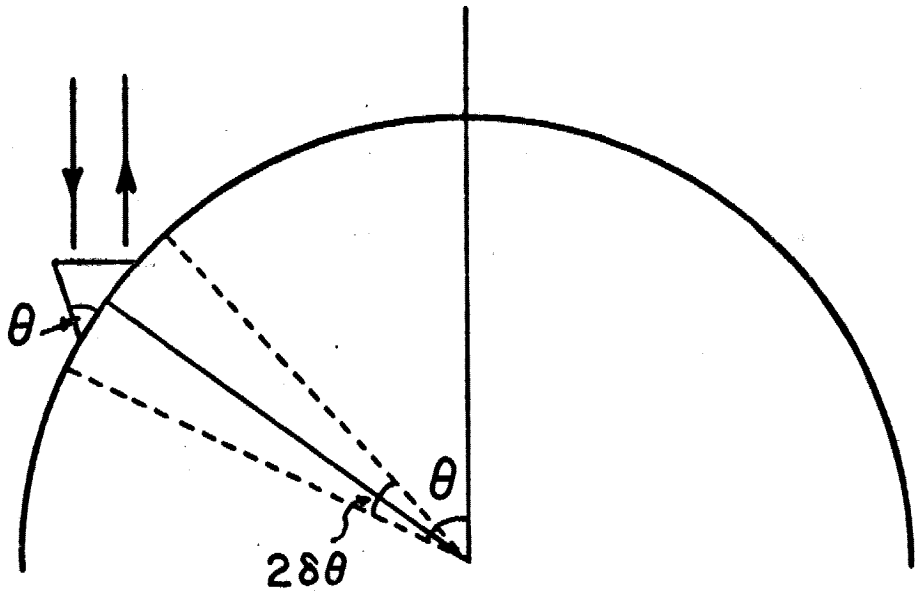


(a)

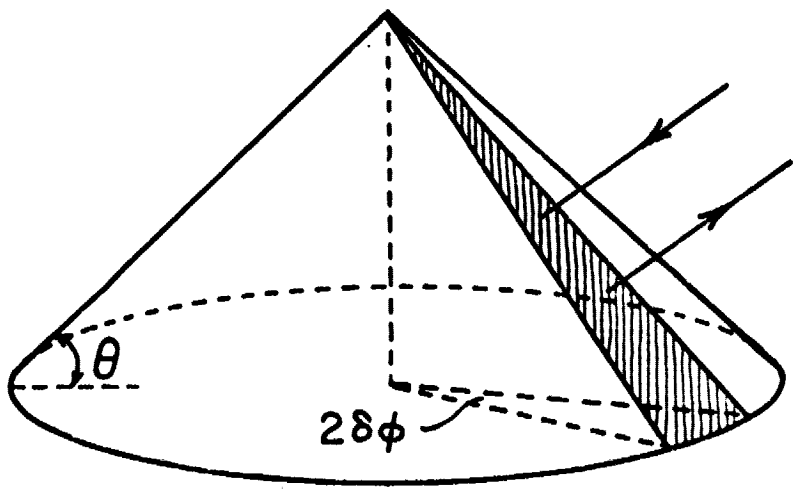


(b)

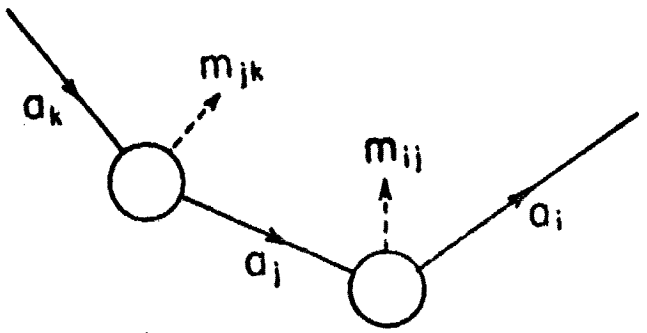
$a_k$
$m_{jk}$
$m_{ij}$
$a_j$
$a_i$

(a)

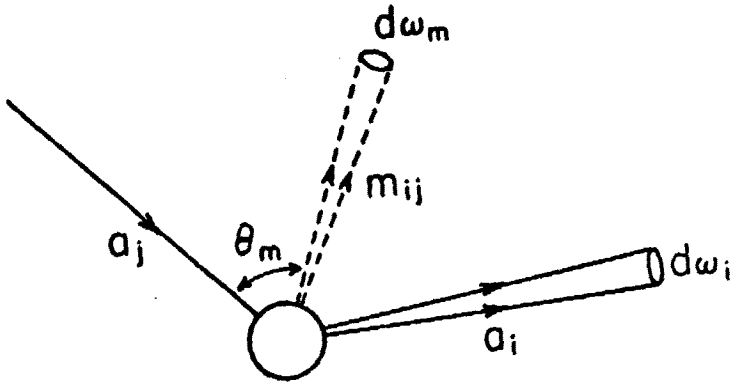
$d\omega_m$
$m_{ij}$
$a_j$
$\theta_m$
$d\omega_i$
$a_i$

(b)

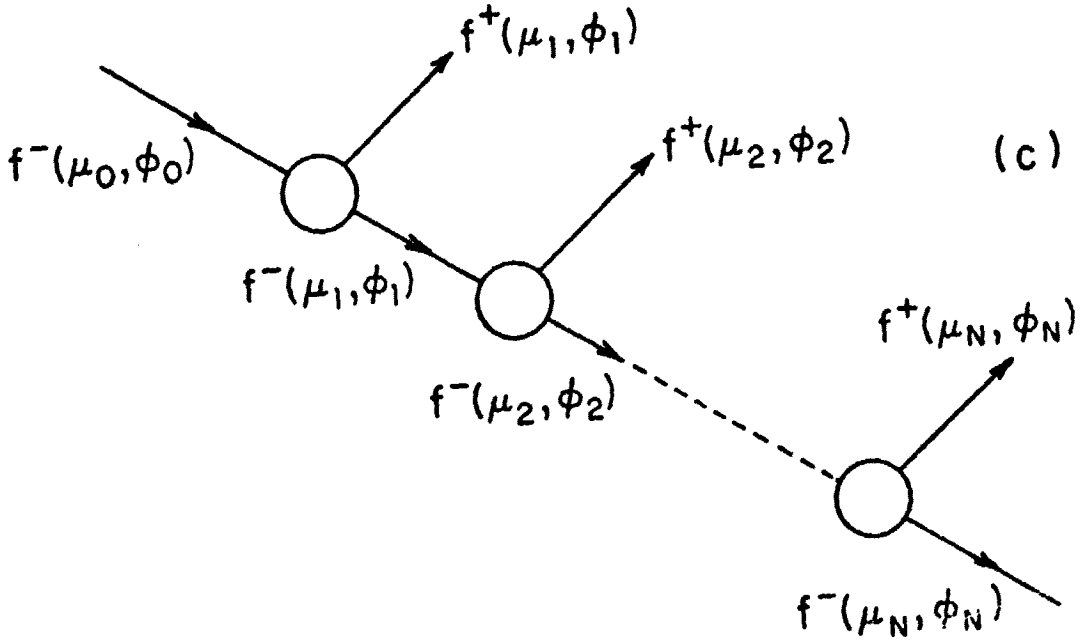
$f^+(\mu_1,\phi_1)$
$f^-(\mu_0,\phi_0)$
$f^+(\mu_2,\phi_2)$
$f^-(\mu_1,\phi_1)$
$f^+(\mu_N,\phi_N)$
$f^-(\mu_2,\phi_2)$
$f^-(\mu_N,\phi_N)$

(c)